Journal of the Iranian Chemical Society
https://doi.org/10.1007/s13738-018-1552-3

ORIGINAL PAPER

Copper(II) Schiff base complex immobilized on graphene nanosheets: a heterogeneous catalyst for epoxidation of olefins

Ali Zarnegaryan[2] · Zari Pahlevanneshan[1] · Majid Moghadam[1] · Shahram Tangestaninejad[1] · Valiollah Mirkhani[1] · Iraj Mohammdpoor-Baltork[1]

Received: 15 March 2018 / Accepted: 12 November 2018

Abstract

The present paper describes the preparation and characterization of Cu(II) Schiff base complex immobilized onto graphene oxide. The structural and morphological characterization of the heterogeneous catalyst was carried out by different techniques such as Fourier transform infrared and diffuse reflectance UV–Vis spectroscopies, X-ray diffraction, thermogravimetric analysis, nitrogen adsorption–desorption, transmission electron microscopy, field emission scanning electron microscopy and inductively coupled plasma atomic emission spectroscopy. The catalytic activity of the heterogeneous catalyst was studied in the epoxidation of various alkenes using *tert*-butyl hydroperoxide as an oxidant and it showed high selectivity and catalytic reactivity. The graphene-bound copper Schiff base was successfully reused for several runs without significant loss in its catalytic activity.

Keywords Graphene nanosheets · Cu(II) Schiff base · Olefin epoxidation · TBHP · Heterogeneous catalyst

Introduction

Epoxidation of alkenes catalyzed by metal complexes is an important reaction in organic synthesis because these compounds serve as useful intermediates that can be used for synthesis of a wide variety of other compounds [1–3]. In recent years, heterogenization of homogeneous catalysts has attracted much attention because they combine the best properties of both homogeneous and heterogeneous catalysts [4]. Among the various approaches for immobilizing soluble catalysts, covalent attachment has been the most frequently used strategy, as the resulting heterogeneous catalysts have good stability during the course of catalytic reactions. The stable covalent bonds reduce the catalyst leaching from the support and thus provide an efficient approach to prepare site-isolated catalysts [5]. Metal Schiff base complexes are of great importance in the coordination chemistry because of their stability, structural variability, ease of preparation and a variety of applications [6, 7]. However, difficult recovery and non-recyclability of these catalysts make them undesirable for large-scale applications. Supported Schiff base complexes have been used for oxidation of olefins and other substances. Many methods and strategies have been reported to immobilize the homogeneous catalysts on insoluble supports such as (i) encapsulation in zeolites, clay or siloxane membranes, (ii) covalent grafting onto inorganic supports such as silica or MCM-41, (iii) co-polymerization of a functionalized salen monomer into an organic polymer, (iv) attachment or build-up of a salen structure to a performed polymer, (v) and axial ligation to surface bound ligands [8–18]. Nowadays, graphene has attracted much attention due to its novel and unique properties [19, 20]. Graphene oxide (GO), the product of oxidation of graphite, possesses abundant oxygen-containing functional groups, which not only render GO moderate water dispersibility but also offer reactive sites for further modification [21]. Different chemical reactions have been reported for modifying and subsequently exfoliating single and/or few graphene layers from bulk graphite [22, 23], Graphene oxide-based materials have found various

✉ Majid Moghadam
moghadamm@sci.ui.ac.ir

✉ Shahram Tangestaninejad
stanges@sci.ui.ac.ir

✉ Valiollah Mirkhani
mirkhani@sci.ui.ac.ir

[1] Department of Chemistry, Catalysis Division, University of Isfahan, 81746-73441 Isfahan, Iran

[2] Department of Chemistry, Yasouj University, 75918-74831 Yasouj, Iran

applications including sensors, solar cells, catalysis, and gas storage [24–28]. Covalent modification of graphene involves the reaction of functional molecules and the oxygenated groups on the GO surface such as carboxyl groups at the periphery, and epoxy, hydroxyl, and C=C groups in the basal plane of GO [29]. For example, the basal surface of GO can be functionalized by the nucleophilic ring-opening reaction between the epoxy groups of GO and the amine groups of 1-(3-aminopropyl)-3-methylimidazolium bromide (an ionic liquid) and 3-aminopropyltriethoxysilane (APTS) [30, 31]. GO is one of the most popular supports used in synthetic organic chemistry because its unique nanostructure, high specific surface area with intrinsic low mass, high density of functional groups such as hydroxyl and epoxide groups on both sides of its surface, ready availability, facile functionalization, and excellent mechanical strength [32, 33]. These characteristics make GO as the most promising supports to immobilize various homogeneous materials, including transition metal complexes as well as metal Schiff base complexes for olefin epoxidation [34–41]. For instance, Mungse et al. prepared oxo-vanadium Schiff base covalently anchored onto graphene oxide sheets for oxidation of alcohols [42]. Su et al. reported GO-supported transition metal Schiff base complexes as efficient and recyclable catalysts for epoxidation of styrene [43]. Zhao et al. prepared GO-supported copper(salen) complex for epoxidation of different alkenes [44]. In this work, we wish to report the design and characterization of a Cu(II) Schiff base complex supported on graphene oxide. In this manner, the copper complex of *N,N′*-(1,2-ethanediyl)bis(1-(4-pyridyl)methanimine) was attached to graphene oxide modified with 3-chloropropyltrimethoxysilane. Also, its catalytic activity was investigated in the epoxidation of different alkenes using dichloromethane as solvent and TBHP as oxidant (Scheme 1).

Experimental

Materials and methods

All chemicals were purchased from Merck and Sigma-Aldrich chemical companies and used without purification. FT-IR spectra were obtained as potassium bromide pellets in the range of 400–4000 cm^{-1} with a JASCO 6300D instrument. Diffuse reflectance UV–Vis (DR UV–Vis) spectra were obtained by a JASCO V-670 (190–700 nm) spectrophotometer. The ICP analyses were performed on an ICP-Spectrociros CCD instrument. The XRD measurements were carried out using a Bruker D8-advance X-ray diffractometer with Cu Kα radiation ($\lambda = 1.5406$ Å). The TEM images were taken using a Philips CM10 instrument. Thermogravimetric analyses (TGA) of the samples were carried out using a STA (model: 6000 Perkin-Elmer, The Netherlands). TGA analyses were performed by heating at a constant rate of 10 °C min^{-1} from 50 to 900 °C under argon atmosphere. The yields were determined by a Shimadzu GC-16A gas chromatograph (GC) equipped with a flame ionization detector. In GC experiments, *n*-decane was used as internal standard. Scanning electron microscopy (SEM) images were obtained using a Hitachi S-4800 field emission scanning electron microscope (FE-SEM) and iridium (IXRF Systems) software. N2 adsorption desorption isotherm, Brunauer–Emmett–Teller (BET) surface area, pore volume, pore diameter and other surface properties of samples were obtained by a Micromeritics instrument (Chem. Bet-3000). The copper loading of the catalyst was determined using an inductively coupled plasma atomic emission spectrometer (ICP-AES). Graphene oxide (GO) was oxidized from graphite powder by a modified Hummer method [45].

The functionalized GO, GO-CP, was prepared by functionalization of GO with 3-chloropropyltrimethoxysilane (CPTMS) as previously reported [44]. The Schiff base ligand, *N,N′*-(1,2-ethanediyl)bis(1-(4-pyridyl)methanimine), was prepared as described in the literature [46].

Synthesis of Schiff base@GO-CP

The GO-CP (500 mg) was dispersed in toluene (100 ml) with vigorous stirring for 30 min. Then, Schiff base ligand (1000 mg) was added to this mixture and the resulting mixture was refluxed for 24 h under nitrogen protection to execute the reaction between chloro groups of CPTMS moieties and nitrogen atoms Schiff base ligand. After the end of the reaction, the solid materials were collected by filtration,

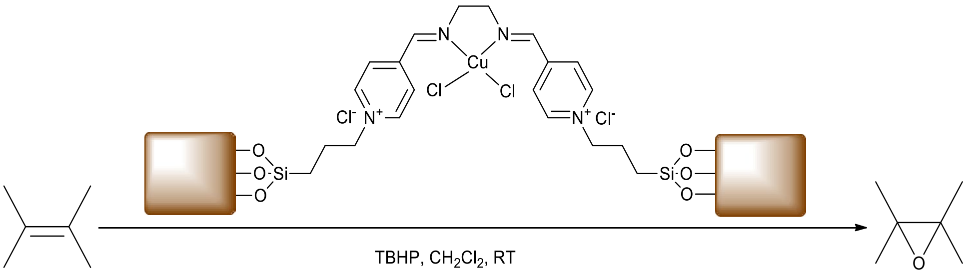

Scheme 1 Alkene epoxidation with TBHP catalyzed by Cu^{II}(Schiff base)Cl_2@GO-CP

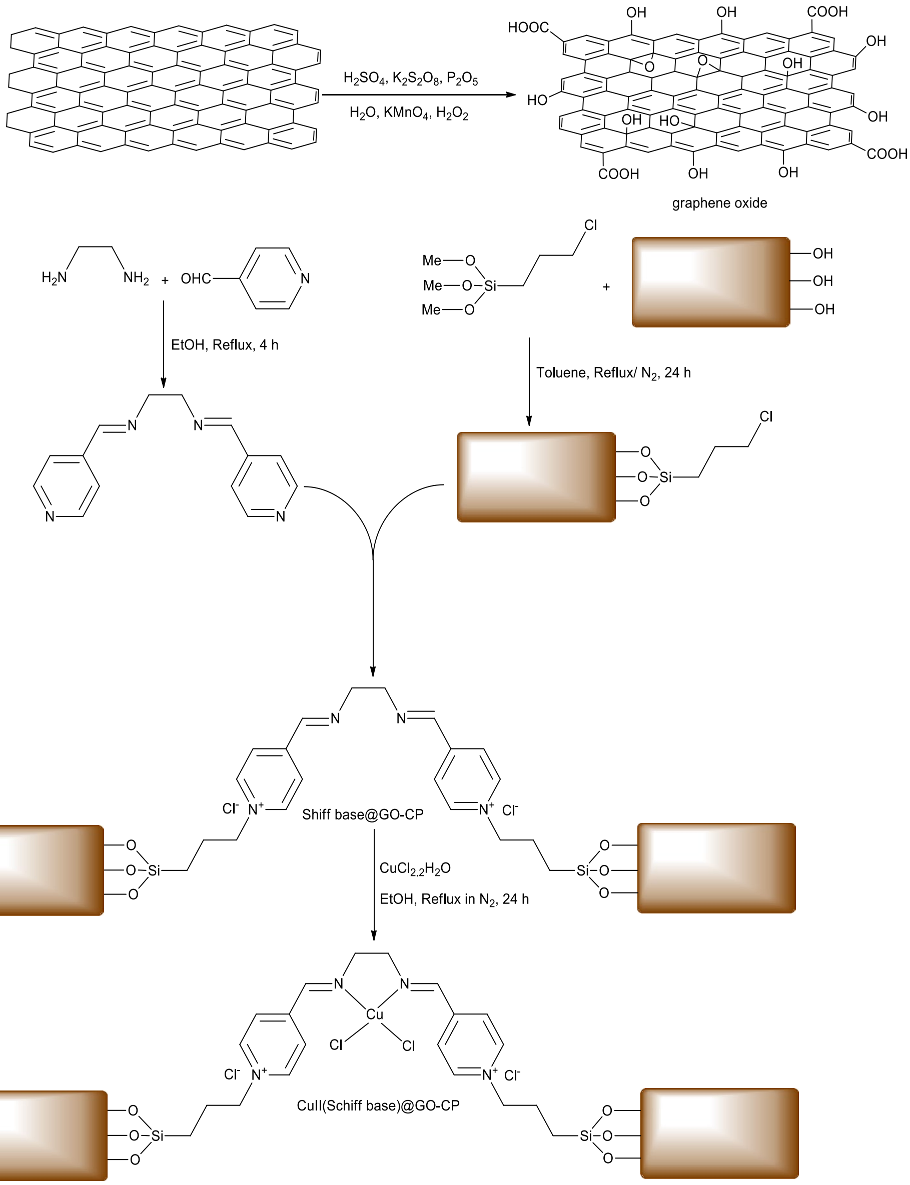

Scheme 2 Preparation of the heterogeneous catalyst

washed with toluene, CH_2Cl_2 successively to remove the unreacted Schiff base ligand.

Immobilization of copper Schiff base on GO-CP

The Schiff base@GO-CP (600 mg) was dispersed in ethanol (50 ml) and refluxed for 12 h in the presence of $CuCl_2$ (200 mg) under a nitrogen atmosphere. After reaction completion, the product was washed with ethanol (4 × 10 ml) to remove the unreacted copper(II) chloride. The final product was dried in an oven. This black powder, graphene oxide-immobilized copper Schiff base, Cu^{II}(Schiff base)Cl_2@GO-CP, was used as a catalyst for the epoxidation of olefins.

General procedure for catalytic epoxidation of olefins with TBHP

To a mixture of alkene (1 mmol) and Cu^{II}(Schiff base)Cl_2@GO-CP catalyst (45 mg, 0.01 mmol) in dichloromethane (5 ml), TBHP (2 mmol) was added and stirred at room temperature. Progress of the reaction was monitored by GC. After completion of the reaction, the catalyst was separated by centrifugation, washed with dichloromethane, and dried at 50 °C. The recovered catalyst was used for investigation of the catalyst reusability.

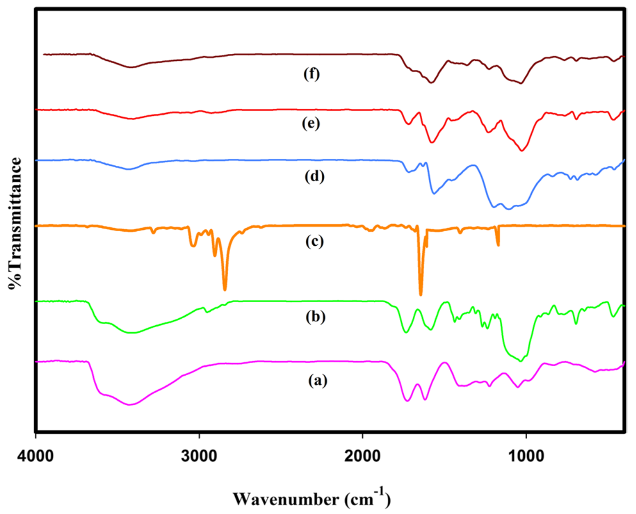

Fig. 1 FT-IR spectra of **a** GO, **b** GO-CP, **c** Schiff base ligand, **d** Schiff base @GO-CP, **e** heterogeneous catalyst and **f** recycled of the heterogeneous catalyst

Results and discussion

Synthesis and characterization of catalyst

3-Chloropropyltrimethoxysilane (CPTMS), which is a coupling agent to attach the complexes on the surface of GO [47–49], was used for anchoring the Cu^{II}(Schiff base) complex on GO. First, 3-chloropropyltrimethoxysilane was grafted on graphene nanosheets by chemical interaction between methoxy groups of CPTMS and hydroxyl groups available on graphene oxide. The Schiff base ligand was attached to GO-CP with via C–N bond. Finally, the copper complex was prepared by the reaction of GO-CP-supported Schiff base with copper(II) chloride (Scheme 2). The copper content of the catalyst, measured by ICP, was found to be 0.23 mmol g^{-1}.

The FT-IR spectra of GO, GO-CP, Schiff base ligand and Cu^{II}(Schiff base)complex@GO-CP catalyst are shown in Fig. 1. In the FT-IR spectrum of GO (Fig. 1a), the strong band at 1726 cm^{-1} (C=O) represents carboxylic acid, and the bands at 1051, 1223 and 1618 cm^{-1} are attributed to the C–O (epoxy), C–OH and C=C groups in graphene oxide, respectively [42].

In addition, a broad band at 3429 cm^{-1} is attributed to the stretching mode of O–H bonds, revealing the presence of many hydroxyl groups. After modification of GO with CPTMS, the bands at 1130 and 1037 cm^{-1} illustrate the presence of Si–O–Si and Si–O–C bonds, respectively. Also, the bands at 2880 and 2920 cm^{-1} are corresponded to the aliphatic C–H bonds. The appearance of these new bands indicates the successful grafting of CPTMS on graphene oxide nanosheets through chemical bonding (Fig. 1b). The FT-IR spectra of the ligand Schiff base (Fig. 1c) showed a strong band at 1644 cm^{-1} which is assigned to stretching vibration of C=N group. These observations confirm the successful grafting of the copper Schiff base complex onto graphene oxide nanosheets by covalent interaction. This band shifts to lower frequency (35 cm^{-1}) in Cu(II) complex which proved the coordination of Cu to Schiff base [50, 51]. The new stretching vibration bands at 2927, 2876, 1578 and 1230 cm^{-1} suggest the grafting of Cu(II) complex on the GO-CP (Fig. 1e). In comparison with the IR spectrum of GO, the relative intensity for C=O decreased and a shift of peak for O–H vibration was observed for the Schiff base@GO-CP heterogeneous catalyst (Fig. 1d). The change in intensity might be indicated as a possible evidence for carboxylic acid coordination of Cu (II) ion [52, 53]. The nature of recovered catalyst was investigated by FT-IR spectroscopy. As can be seen, the FT-IR spectrum of the reused catalyst is similar to

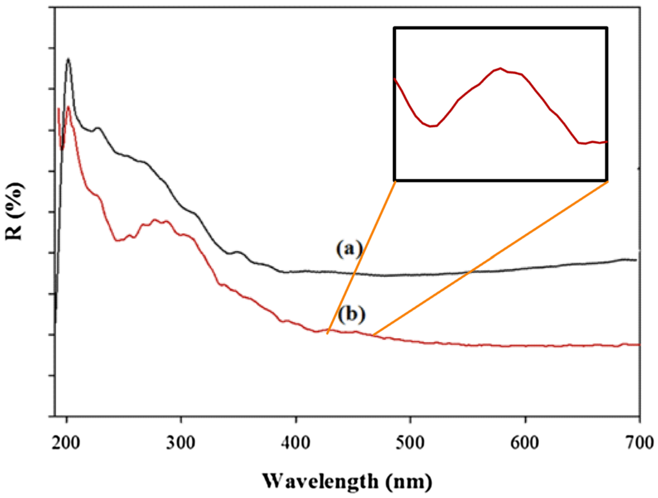

Fig. 2 UV–Vis spectra of **a** GO, **b** Cu(II)(Shiff-base)@GO-CP catalyst

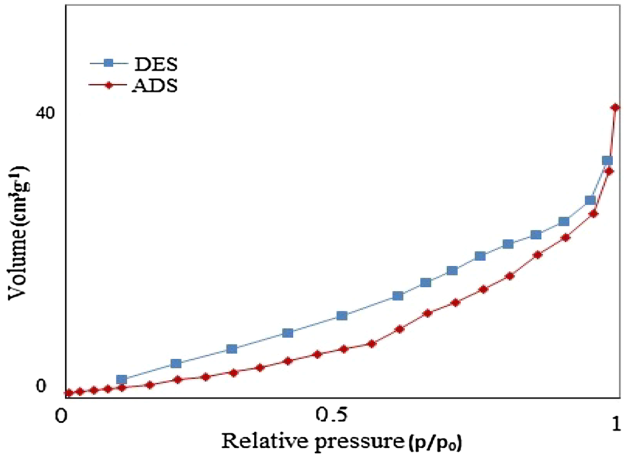

Fig. 3 Nitrogen adsorption–desorption of heterogeneous catalyst

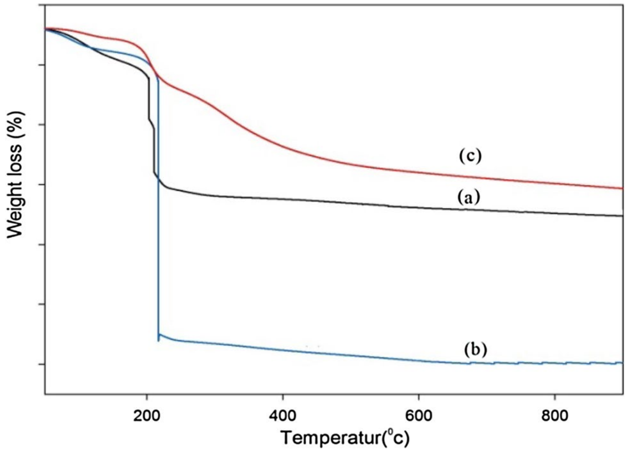

Fig. 4 The TG curves of **a** GO, **b** GO-CP, and **c** heterogeneous catalyst

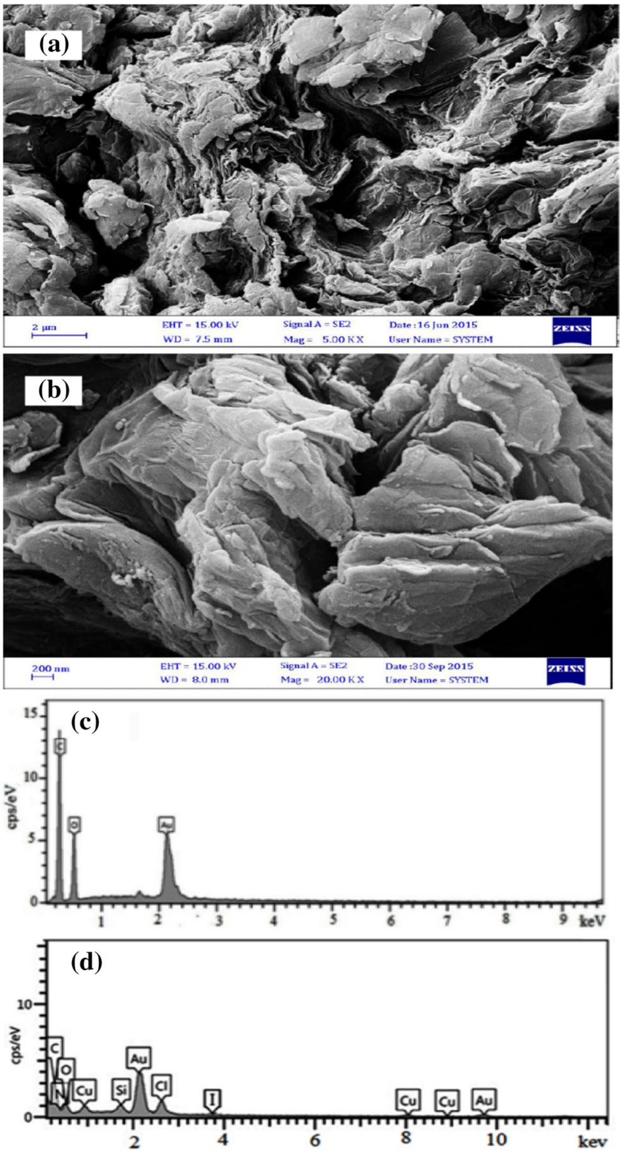

Fig. 5 FE-SEM images of **a** GO and **b** heterogeneous catalyst and EDX spectrum of: **c** GO and **d** heterogeneous catalyst

fresh catalyst which shows the stability of the reused catalyst during the catalytic cycles (Fig. 1f).

The diffuse reflectance UV–Vis spectra of GO and Cu^{II}(Schiff base)Cl_2@GO-CP catalyst are shown in Fig. 2. The UV–Vis spectrum of GO shows a strong absorption peak at 224 nm owing to discrete units of sp^2-bonded carbons [54] and an absorption peak shoulder at around 300 nm, which are attributed to n–π* transition of C=O bonds (Fig. 2a) [42]. In addition, the absorption bands observed in the 280–330 nm region can be assigned to the n → π* and π → π* ligand charge transfer in Cu^{II}(Schiff base) Cl_2@GO-CP [55]. The very weak bands at ca. 450 nm may be attributed to *d*–*d* transitions of the centred Cu ion, supporting the immobilization of Cu^{II}(Schiff base)Cl_2 on GO.

BET surface area, pore diameter and pore of the Cu^{II}(Schiff base)Cl_2@GO-CP were measured using nitrogen adsorption–desorption isotherms at 77 K (Fig. 3). The nitrogen adsorption–desorption analysis of heterogeneous catalyst showed a type V isotherm and H_1 hysteresis loop with intensity lower than its parent (Fig. 3). The BET surface area and total pore volume of the Cu^{II}(Schiff base)@GO were decreased to 15.79 $m^2\ g^{-1}$ and 0.066, $cm^3\ g^{-1}$, respectively. The mean pore diameter of the catalyst was also found to be 16.81 nm according to BJH method [56].

The TGA curves of GO, GO-CP and heterogeneous catalyst in the range of 50–900 °C and a heating rate of 10 °C min^{-1} under air atmosphere are shown in Fig. 4. Graphene oxide shows a low weight loss (3.5 wt%) below 100 °C, evidently owing to evaporation of water molecules which are held in the material. The second significant weight loss is observed around 200 °C, due to decomposition of the labile

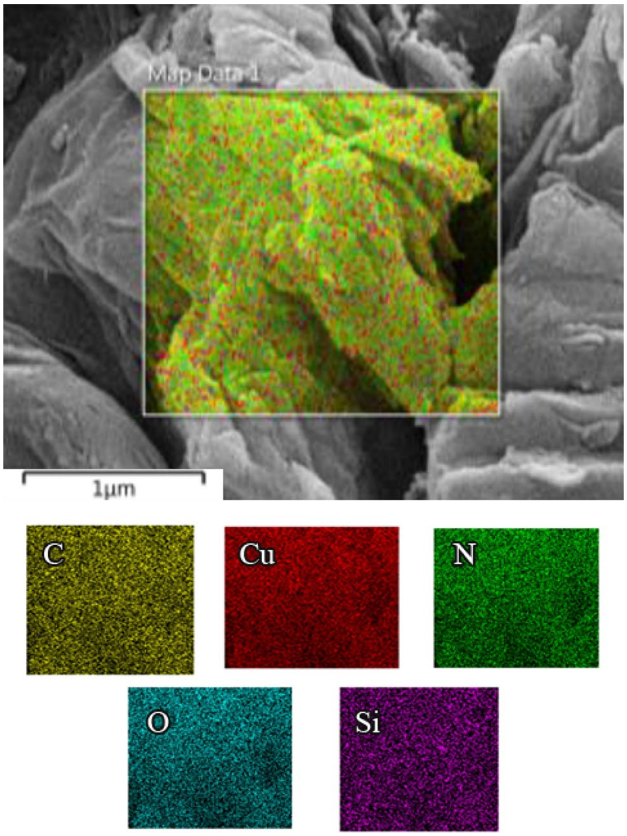

Fig. 6 Elemental mapping images of heterogeneous catalyst

oxygen-containing functional groups, yielding CO, CO_2, and steam, and the latter is attributed to pyrolysis of the carbon skeleton of GO (Fig. 4a) [57, 58]. After chemical functionalization of GO with CPTMS, the GO-CP shows gradual weight loss in the temperature range of 140–180 °C and significant weight loss around 210 °C. The former can be attributed mostly to the COOH (undigested oxygen carrying functionalities) groups that are incomplete dearomatized, which have not participated in interaction with CPTMS (Fig. 4b) [57]. The thermogram of the graphene-immobilized copper Schiff base catalyst illustrates an exothermic major weight loss over a wide range of temperature (180–450 °C) on account of slow decomposition of the Schiff base complex (Fig. 4c) [43].

The morphologies of the surface GO and Cu^{II}(Schiff base)Cl_2@GO-CP were studied by field emission scanning electron microscopy (FE-SEM). As shown in (Fig. 5a), there are large flakes of GO with macroscopic wrinkling. Compared to GO sheets, the FE-SEM image of Cu^{II}(Schiff base)Cl_2@GO-CP (Fig. 5b) exhibited an agglomerated layered structure incorporating copper complex moieties between the sheets. The energy dispersive X-ray spectroscopy (EDX) analysis of GO (Fig. 5c) showed that the major elements are carbon and oxygen. In the EDX spectrum of Cu^{II}(Schiff base)Cl_2@GO-CP (Fig. 5d), the presence of Cu, N and Cl peaks originates from Cu^{II}(Schiff base)Cl_2 which is a good indication in for attachment of Cu^{II}(Schiff base)Cl_2 to GO-CP sheets.

The corresponding elemental mapping of the heterogeneous catalyst was also performed to understand the distribution of the copper Schiff base complex on GO-CP. As can be seen, all carbon, oxygen, silicon, nitrogen and copper elements have uniform distribution in the catalyst texture which showed successful immobilization of the catalyst on GO-CP (Fig. 6).

The texture of the catalyst was also studied by transmission electron microscopy (TEM). The TEM image of GO shows transparent stacked sheets while the TEM image of the Cu catalyst (Fig. 7) shows evenly distributed dark spots, which are probably due to the attachment of the Cu^{II}(Schiff base)Cl_2 onto GO.

The XRD patterns are used to study the changes in structure (Fig. 8). For GO, two peaks at $2\theta = 11.3°$ and 24.26° correspond to (001) and (002) reflections of GO and graphite powder, respectively (Fig. 8a) [42]. After immobilization of CP on GO, a broad peak appeared at around $2\theta = 21°$ which corresponds to amorphous silica (Fig. 8b) [59]. By immobilization of Cu^{II}(Schiff base)Cl_2, the diffraction peaks become

Fig. 7 TEM images of heterogeneous catalyst

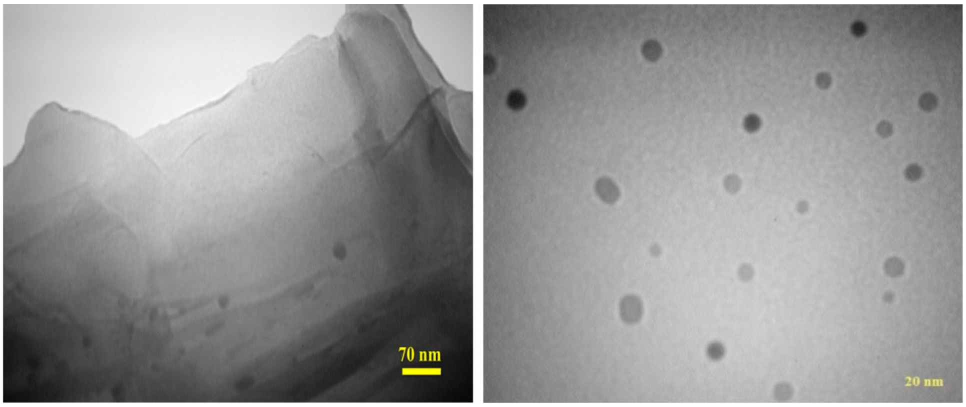

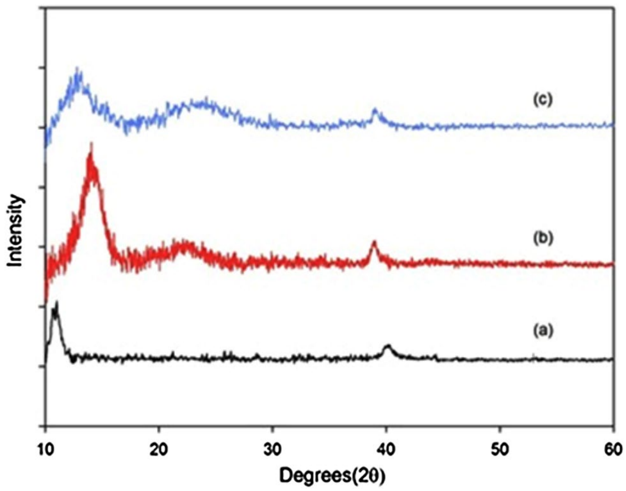

Fig. 8 XRD patterns of **a** GO; **b** GO–CP and **c** heterogeneous catalyst

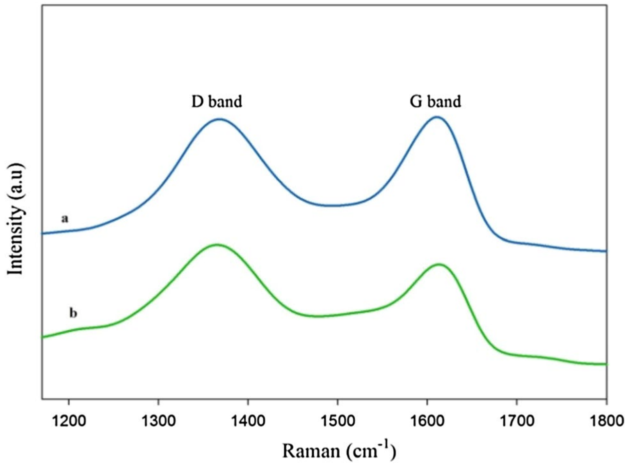

Fig. 9 Raman spectra of **a** GO and **b** Cu^{II}(Schiff base)Cl$_2$@GO-CP catalyst

Table 1 Optimization of reaction conditions in the epoxidation of cyclooctene at room temperature

Entry	Solvent	Catalyst (mol%)	Yield (%)[a]
1	EtOAc	1	78
2	CH_3CN	1	88
3	MeOH	1	51
4	THF	1	45
5	EtOH–H_2O	1	32
6	$C_2H_4Cl_2$	1	48
7	H_2O	1	20
8	CH_2Cl_2	1	99
9	CH_2Cl_2	1.25	99
10	CH_2Cl_2	0.75	76
11	CH_2Cl_2	0.5	54
12	CH_2Cl_2	0.25	28
13	CH_2Cl_2	0	5

Reaction conditions: cyclooctene (1 mmol), TBHP (2 mmol), catalyst

[a] Determined by GC based on the starting cyclooctene, after 5 h

weak and broad at around $2\theta = 11.91°$, indicating that the mentioned catalyst has been successfully prepared (Fig. 8c).

The chemical and structural changes in the obtained materials can be also studied by the Raman spectroscopy (Fig. 9). Raman spectra of GO and Cu^{II}(Schiff base)Cl$_2$@GO-CP exhibit the presence of two characteristic G and D bands. The band at 1354 cm^{-1} (D) is attributed to the amount of defects existing in the carbon framework, and the band at 1597 cm^{-1} (G) corresponds to the E$_2$g mode of hexagonal sp^2 carbon domains, representing the degree of graphitization [60, 61]. The intensity ratio between the D and G bands (I_D/I_G ratio) indicates the degree of defects, ripples, edge, and the average size of sp^2 domains [62]. At Fig. 9b, the peaks at 1357 and 1602 cm^{-1} can be attributed to the D and G bands of the Cu^{II}(Schiff base)Cl$_2$@GO-CP. The ratio increased very small from GO to Cu^{II}(Schiff base) @GO-CP, indicating the successful covalent attachment of Cu^{II}(Schiff base)Cl$_2$ complex to the GO support.

Investigation of catalytic activity of Cu^{II}(Schiff base)Cl$_2$@GO-CP in the epoxidation of alkenes

The catalytic activity of the Cu^{II}(Schiff base)Cl$_2$@GO-CP was studied in the epoxidation of alkenes with *tert*-BuOOH as an oxidant. First, the epoxidation of cyclooctene with *tert*-butyl hydroperoxide was chosen to optimize the reaction parameters such as catalyst amount and solvent. Different solvents such as dichloromethane, ethyl acetate, acetonitrile, methanol, ethanol, tetrahydrofuran (THF), ethanol–water, 1,2-dichloroethane and water were studied for optimization of the solvent in the epoxidation of cyclooctene with TBHP. As can be seen, dichloromethane is the best reaction medium (Table 1, entries 1–8). Different amounts of heterogeneous catalyst (0.25–1.25 mol% based on Cu loading) were also used in the model reaction. By increasing the amount of catalyst from 0.25 to 1 mol%, the yield was increased from 28 to 99%. Increasing the amount of catalyst did not show any significant effect on the epoxide yield at room temperature (Table 1, entry 8–12). It is noteworthy that in the absence of catalyst, only small amount of epoxide was detected even after prolonged reaction time (Table 1, entry 13). Under the optimized reaction conditions, different molar ratio of olefin/TBHP was used and the best results were obtained with 2 mmole of TBHP.

Table 2 Epoxidation of alkenes with TBHP catalyzed by heterogeneous Cu(II) complex at room temperature

Entry	Olefin	Product	Yield (%)[a]	Epoxide Selectivity (%)	TOF (h^{-1})
1	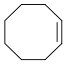	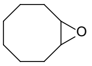	99	100	19.1
2	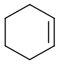	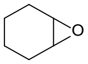	94	97[b]	18.2
3	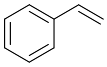	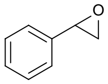	90	91[c]	16.4
4	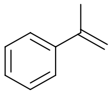	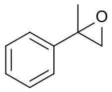	87	93[d]	15.8
5	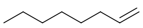	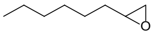	80	100	15.4
6	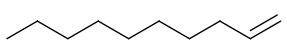	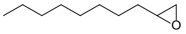	78	100	15.1
7[e]	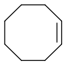	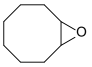	43	100	8.6

a

Reaction conditions: alkene (1 mmol), TBHP (2 mmol) and heterogeneous Cu(II) complex catalyst (1 mol% based on Cu) in dichloromethane at room temperature after 5 h

[a] Determined by GC based on starting alkene

[b] The by-product is cyclohex-2-ene-1-one

[c] The by-product is benzaldehyde

[d] The by-product is acetophenone

[e] Reaction conditions: alkene (1 mmol), TBHP (2 mmol) and Cu(II) Schiff base complex (1 mol% based on Cu) in dichloromethane at room temperature after 5 h

To expand the scope and generality of this catalytic system, different alkenes including cyclic and linear ones were subjected to epoxidation with TBHP at room temperature in CH_2Cl_2. The results are summarized in Table 2. In general, the cyclic alkenes and the alkenes containing aromatic ring were more reactive (Table 2, entries 1–4) than linear ones (Table 2, entries 5 and 6). Excellent conversion and selectivity to the epoxide were obtained within 5 h (Table 2, entries 1–6). Cyclic olefins such as cyclohexene and cyclooctene were also epoxidized in high yields and selectivity (Table 2, entries 1 and 2). While in the case of the terminal C=C double bonds conjugated with an aromatic ring, the major product was the corresponding epoxide and the related carbonyl compound was achieved as a by-product resulting from ring-opening reaction of epoxide (Table 2, entries 3 and 4). 1-Octene and 1-decene as linear alkenes were epoxidized efficiently by this catalyst in high yields. For comparison, the catalytic performance of homogeneous Cu(II) Schiff base complex was also investigated in cyclooctene epoxidation in the same reaction condition (Table 2, entry 7). As can be seen, the catalytic activity of the homogeneous Cu(II) Schiff base catalyst is significantly lower than the heterogeneous Cu(II) catalyst which confirms that graphene oxide anchoring plays an influential role in catalytic efficiency. According to the related literature [43], a possible mechanism was suggested for alkene epoxidation with copper(II) complex using TBHP that we can also consider it in the current study.

Recently, we reported a heterogeneous copper catalyst in the alkene epoxidation [63]. This catalytic system showed slightly higher catalytic activity compared to previously reported system. This behaviour can be attributed to the presence of chloropropyl dangling groups and also the presence of supported ionic liquid moieties in which the heterogeneous catalyst acts as a quasi-homogeneous system.

Also, the results obtained using Cu^{II}(Schiff base)Cl_2@GO-CP in the epoxidation of cyclohexene were compared with the results reported for some other copper(II) catalysts. As can be seen, our reported method is superior in terms of reaction times, yields or epoxide selectivity (Table 3).

Table 3 Comparison of the catalytic efficiency of Cu^{II}(Schiff base) complex@GO-CP with other reported copper(II) catalysts for the cyclooctene epoxidation with *tert*-butyl hydroperoxide

Entry	Catalyst	Time (h)	Conversion (%)	Selectivity (%) epoxide	TOF (h^{-1})	References
1	Cu^{II}(Schiff base)@GO-CP	5	99	100	19.1	This study
2	$[Cu_4(O)(L^2)_2(CH_3COO)_4]CH_3CN$	24	88	89	4.4	[64]
3	LCu^{II}	24	78	60	13	[65]
4	$LCu^{I}Cu^{II}$	24	74	57	12.3	[65]
5	$Cu\{salnptn(3\text{-}OMe)_2\}$	24	70	26	12.8	[66]
6	Cu{hnaphnptn}	24	70	24	12.5	[66]
7	CuO	24	64	100	0.3	[67]
8	$[CuL(\mu_{1,1}, N_3)]_n$	24	86	81	6.8	[68]
9	$[Cu_2(L)_2(L^3)]PF_6$	22	50	50	24	[69]
10	Cu(salen)-f-GO	12	52.8	43.6	69.6	[44]
11	Cu-AMM	24	92	93	65.4	[70]
12	$Cu^{II}(BAPTE)Cl_2$@GO	8	97	100	17.3	[63]

Also, in most cases, higher TOFs have been obtained by our reported method.

Reusability of the catalyst

The reusability of Cu^{II}(Schiff base)Cl_2@GO-CP was tested in the repeated epoxidation reactions of cyclooctene. In this manner, after each reaction, the solid catalyst was easily recovered from the reaction mixture by simple filtration or centrifugation, and washed with CH_2Cl_2 and reused with fresh reactants. The filtrates were used for determination of the amount of Cu leached by ICP analysis. No copper was detected in the filtrates which showed the strong attachment of the Cu Schiff base to the functionalized GO. After using the catalyst for five consecutive runs, the epoxide yield was still 95% (Fig. 10).

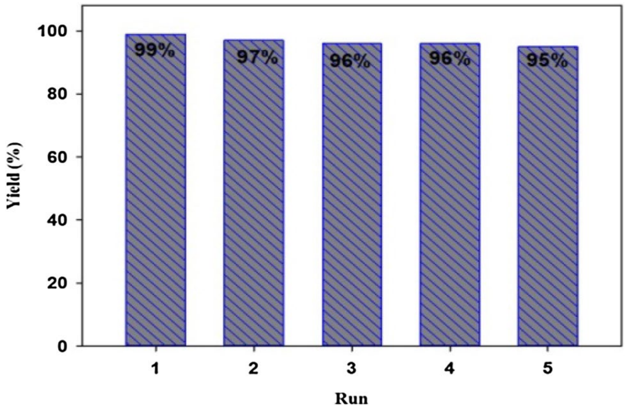

Fig. 10 Reusability of catalyst in the epoxidation of cyclooctene with TBHP at room temperature

Conclusions

In conclusion, a Schiff base ligand was immobilized on GO nanosheets and complexed with Cu(II) species. This immobilized copper Schiff base complex, Cu^{II}(Schiff base)Cl_2@GO-CP, was used as a highly effective and recyclable catalyst for the epoxidation of olefins with TBHP. High yields, excellent selectivity and reusability of the catalyst are noteworthy advantages of this catalytic system.

Acknowledgements The authors are grateful to the Research Council of the University of Isfahan for financial support of this work.

References

1. R.A. Sheldon, J.K. Kochi, *Metal-Catalysed Oxidations of Organic Compounds* (Academic Press, New York, 1981)
2. Q.H. Xia, H.Q. Ge, C.P. Ye, Z.M. Liu, K.-X. Su, Chem. Rev. **105**, 1603 (2005)
3. B. Qi, X.H. Lu, D. Zhou, Q.H. Xia, Z.R. Tang, S.Y. Fang, Y.L. Dong, J. Mol. Catal. A Chem. **322**, 73 (2010)
4. D.E. De Vos, M. Dams, B.F. Sels, P.A. Jacobs, Chem. Rev. **102**, 3615 (2002)
5. P. Roy, M. Nandi, M. Manassero, M. Ricco, M. Mazzani, A. Bhaumik, P. Banerjee, Dalton Trans. **43**, 9543 (2009)
6. M. Torki, S. Tangestaninejad, V. Mirkhani, M. Moghadam, I. Mohammadpoor-Baltork. Appl. Organomet. Chem. **28**, 304 (2014)
7. M. Yadegari, M. Moghadam, S. Tangestaninejad, V. Mirkhani, I. Mohammadpoor-Baltork, Polyhedron **31**, 332 (2012)

8. B. Bahramian, V. Mirkhani, M. Moghadam, S. Tangestaninejad, Catal. Commun. **7**, 289 (2006)
9. V. Mirkhani, M. Moghadam, S. Tangestaninejad, B. Bahramian, A. Mallekpoor-Shalamzari, Appl. Catal. A Gen. **321**, 49 (2007)
10. S. Tangestaninejad, M. Moghadam, V. Mirkhani, I. Mohammadpoor-Baltork, K. Ghani, Catal. Commun. **10**, 853 (2009)
11. S. Tangestaninejad, M. Moghadam, V. Mirkhani, I. Mohammadpoor-Baltork, M.S. Saeedi, Appl. Catal. A Gen. **381**, 233 (2010)
12. M. Zakeri, M. Moghadam, I. Mohammadpoor-Baltork, S. Tangestaninejad, V. Mirkhani, A.R. Khosrpour, M. Alizadeh, Transit. Met. Chem. **37**, 45 (2012)
13. W.R. Lazar. Thiel, A.P. Singh, RSC Adv. **4**, 14063 (2014)
14. A. Bezaatpour, S. Khatami, M. Amiri, RSC Adv. **6**, 27452 (2016)
15. M. Jafarpour, H. Kargar, A. Rezaeifard, RSC Adv. **6**, 79085 (2016)
16. M. Asadniaye Fardjahromi, M. Moghadam, S. Tangestaninejad, V. Mirkhani, I. Mohammadpoor-Baltork, RSC Adv., **6**, 20128 (2016)
17. V. Visnja, P. Jana, P. Biserka, A. Dominique, N. Predrag, M. Dubravka, RSC Adv. **6**, 36384 (2016)
18. W. Wang, D. Agustin, R. Poll, J. Mol. Catal. **443**, 52 (2017)
19. K. S.Novoselov, A. K.Geim, S. V.Morozov, D.Jiang, Y.Zhang, S. V.Dubonos, I. V.Grigorieva, A. A.Firsov, Science **306**, 666 (2004)
20. A.K. Geim, K.S. Novoselov, Nat. Mater. **6**, 183 (2007)
21. D.R. Dreyer, S. Park, C.W. Bielawski, R.S. Ruoff, Chem. Soc. Rev. **39**, 228 (2010)
22. S. Park, R.S. Ruoff, Nat. Nanotechnol **4**, 217 (2009)
23. K.P. Loh, Q. Bao, P.K. Ang, J. Yang, J. Mater. Chem. **20**, 2277 (2010)
24. S. Stankovich, D.A. Dikin, G.H.B. Dommett, K.M. Kohlhaas, E.J. Zimney, E.A. Stach, R.D. Piner, S.T. Nguyen, R.S. Ruoff, Nature **442**, 282 (2006)
25. C.H. Lu, H.H. Yang, C.L. Zhu, X. Chen, G.N. Chen, Angew Chem. Int. Ed. **48**, 4785 (2009)
26. Y.H. Hu, H. Wang, B. Hu, ChemSusChem **3**, 782 (2010)
27. J. Pyun, Angew Chem. Int. Ed. **50**, 46 (2011)
28. L. Wang, K. Lee, Y.Y. Sun, M. Lucking, Z. Chen, J.J. Zhao, S.B. Zhang, ACS Nano **3**, 2995 (2009)
29. A. Lerf, H. He, M. Forster, J. Klinowski, J. Phys. Chem. B **102**, 4477 (1998)
30. H.F. Yang, C.S. Shan, F.H. Li, D.X. Han, Q.X. Zhang, L. Niu, Chem. Commun. **26**, 3880 (2009)
31. H.F. Yang, F.H. Li, C.S. Shan, D.X. Han, Q.X. Zhang, L. Niu, A. Ivaska, J. Mater. Chem. **19**, 4632 (2009)
32. D.A. Dikin, S. Stankovich, E.J. Zimney, R.D. Piner, G.H.B. Dommett, G. Evmenenko, S.T. Nguyen, R.S. Ruoff, Nature **448**, 457 (2007)
33. O.C. Compton, S.T. Nguyen, Small **6**, 711 (2010)
34. L. Dong, R.R.S. Gari, Z. Li, M.M. Craig, S. Hou, Carbon **48**, 781 (2010)
35. T.A. Pham, B.C. Choi, Y.T. Jeong, Nanotech **21**, 465603 (2010)
36. M. Moghadam, H. Salavati, Z. Pahlevanneshan, J. Iran. Chem. Soc. **15**, 529 (2018)
37. L. Zhifang, W. Shujie, D. Hong, Z. Dafang, H. Jing, W. Xu, H. Qisheng, G. Jingqi, K. Qiubin, New J. Chem. **37**, 1561 (2013)
38. S. Rayati, E. Khodaei, S. Shokoohi, M. Jafarian, B. Elmi, A. Wojtczak, Inorgan. Chim. Acta **466**, 520 (2017)
39. A. Allahresani, J. Iran. Chem. Soc. **14**, 1051 (2017)
40. A. Zarrinjahan, M. Moghadam, V. Mirkhani, S. Tangestaninejad, I. Mohammadpoor-Baltork, J. Iran. Chem. Soc. **13**, 1509 (2016)
41. S. Tangestaninejad, M. Moghadam, V. Mirkhani, I. Mohammadpoor-Baltork, K. Ghani, Iran. Chem. Soc. **5**(Supplement 1), S71–S79 (2008)
42. H.P. Mungse, S. Verma, N. Kumar, B. Sain, O.P. Khatri, J. Mater. Chem. **22**, 5427 (2012)
43. H. Su, Z. Li, Q.I. Guo, J.I. Guang, Q. Kan, RSC Adv. **4**, 9990 (2014)
44. Q. Zhao, C. Bai, W. Zhang, Y. Li, G. Zhang, F. Zhang, X. Fan, Ind. Eng. Chem. Res. **53**, 4232 (2014)
45. W.S. Hummers, R.E. Offeman, J. Am. Chem. Soc. **80**, 1339 (1957)
46. P.K. Pal, S. Chowdhury, P. Purkayastha, D.A. Tocher, D. Datta, Inorg. Chem. Commun. **3**, 585 (2000)
47. M. Lazghab, K. Saleh, P. Guigon, Chem. Eng. Res. Des. **88**, 686 (2010)
48. C. Baleizao, B. Gigante, M.J. Sabater, H. Garcia, Appl. Catal. A Gen. **228**, 279 (2002)
49. B. Jarrais, C. Pereira, A. Rosa Silva, A.P. Carvalho, J. Pires, C. Freire, Polyhedron **28**, 994 (2009)
50. Y. Gao, Y. Zhang, C. Qiu, J. Zhao, Appl. Organomet. Chem. **25**, 54 (2011)
51. D. Nunes, M. Pillinger, A.A. Valente, I.S. Goncalves, J. Rocha, P. Ferreira, F.E. Kuhn, Eur. J. Inorg. Chem. 2002, 1100
52. M. Mathesh, J. Liu, N.D. Nam, S.K. Lam, R. Zheng, C.J. Barrow, W. Yang, J. Mater. Chem. C **18**, 3084 (2013)
53. S. Park, K.S. Lee, G. Bozoklu, W. Cai, S.T. Nguyen, R.S. Ruoff, ACS Nano **2**, 572 (2008)
54. P.K. Khatri, S. Choudhary, R. Singh, S.P. Jain, C. Khatri, Dalton Trans. **43**, 8054 (2014)
55. V.H. Pham, T.V. Cuong, S.H. Hur, E.W. Shin, J.S. Kim, J.S. Chung, E.J. Kim, Carbon **48**, 1945 (2010)
56. P. Kumar, G. Singh, D. Tripathi, S.L. Jain, RSC Adv. **4**, 50331 (2014)
57. V. León, M. Quintana, M.A. Herrero, J.L.G. Fierro, A. delaHoz, M. Prato, E. Vázquez, Chem. Commun. **47**, 10936 (2011)
58. H.X. Wang, K.G. Zhou, Y.L. Xie, J. Zeng, N. NaChai, J. Li, H.L. Zhang, Chem. Commun. **47**, 5747 (2011)
59. M.A. Nasseri, A. Allahresani, H. Raissi, RSC Adv. **4**, 26087 (2014)
60. F. Tuinstra, J.L. Koenig, J. Chem. Phys. **53**, 1126 (1970)
61. G. Venugopal, M.H. Jung, M. Suemitsu, S.J. Kim, Carbon **49**, 2766 (2011)
62. A.C. Ferrari, J.C. Meyer, V. Scardaci, C. Casiraghi, M. Lazzeri, F. Mauri, S. Piscanec, D. Jiang, K.S. Novoselov, S. Roth, A.K. Geim, Phys. Rev. Lett. **97**, 187401 (2006)
63. A. Zarnegaryan, M. Moghadam, S. Tangestaninejad, V. Mirkhani, I. Mohammdpoor-Baltork, New J. Chem. **40**, 2280 (2016)
64. P. Roy, M. Nandi, M. Manassero, M. Ricco´, M. Mazzani, A. Bhaumik, P. Banerjee, Dalton Trans. **43**, 9543 (2009)
65. S. Biswas, A. Dutta, M. Dolai, I. Bhowmick, M. Rouzières, H.M. Lee, R. Clérac, M. Ali, Eur. J. Inorg. Chem. 2013, 4922
66. S. Rayati, S. Zakavi, M. Koliaei, A. Wojtczak, A. Kozakiewicz, Inorg. Chem. Commun. **13**, 203 (2010)
67. L. Xu, S. Sithambaram, Y. Zhang, C. Chen, L. Jin, R.Joesten and S.L. Suib, Chem. Mater. **21**, 1253 (2009)
68. R. hBera, C. Adhikary, S. Ianelli, S. Chaudhuri, S. Koner, Polyhedron **29**, 2166 (2010)
69. S. Ray, S. Jana, A. Jana, S. Konar, K. Das, S. Chatterjee, R.J. Butcher, S. Kumar Kar, Polyhedron **46**, 74 (2012)
70. M. Nandi, P. Roy, H. Uyamac, A. Bhaumik, Dalton Trans. **40**, 12510 (2011)